Constraint Effects in Creeping Solids Under Biaxial Loading

V.N. Shlyannikov[1,a], N.V. Boichenko[1,b]

[1] Lobachevsky Street, 2/31, post-box 190, Kazan, 420111, Russia

[a] e-mail: shlyannikov@mail.ru, [b] e-mail: tasha1203@mail.ru

Key words: Biaxial loading, higher-order terms, constraint parameter, crack-tip field, plane strain, creeping materials.

Abstract. The method of determination for the higher-order crack-tip fields is elaborated and realized in a power-law creeping material under biaxial loading. The higher-order both stress and strain rate fields and second order amplitude coefficients are obtained. The results of numerical study of stress strain state under biaxial loading at the blunted crack tip on different creep time are presented. Three-dimensional nonlinear finite element analysis was used to determine the variations of a constraint parameter based on the stress invariants and the tangential stress distributions along the crack plane. In this study different concepts utilizing a higher term of power-law hardening crack-tip stress field and the local triaxiality parameter are analyzed numerically with respect to their capability of characterizing in-plane constraint effects. Numerical aspects are investigated in three-dimensional nonlinear elastic-plastic finite element analysis of the biaxially loaded rectangular plate under plane strain conditions. It is found that the near-tip second stress fields are dependent on the magnitude and sign of the nominal biaxial stress ratio. The relation between a dimensionless amplitude factor of the higher-order creep stress field and biaxial stress ratio for different crack tip distance is determined.

Introduction

A three-term generalized asymptotic expansion of the stress function [1,2] were used to describe the stress field in the vicinity of the crack tip in a creeping material and also to interpret the constraint effects due to finite specimen geometry and loading configurations. Although there has been a wide range of studies on the effects of constraint for mode I, at the same time very little research has been reported in the literature concerning of the biaxial loading influence. Most of the above analyses on the constraint effect are focused on the determination of second order term amplitude under uniaxial tension or bending. Thus, the influence of the nominal stress biaxial ratio on dimensionless angular higher-order stress functions has not been studied so far with exception of [3,4] investigations. In particular, it is not clear whether the T-stress is a unique parameter characterizing stress fields in a wide range of biaxial loading configurations under mode I both plane strain and plane stress conditions. Moreover, only limited studies were conducted in the past to study the effect of loading biaxiality on both the higher order crack-tip fields and constraint parameter behavior for creeping materials.

Three-term asymptotic solution

One of the purposes of our work is to reveal the asymptotic results that can accurately characterize the fields near a crack tip in creeping materaials. It should be noted that creep fracture mechanics has often relied on the straightforward application of the Hoff analogy [5] by which the HRR solution for power-law creeping materials can be obtained by replacing the J-integral by $C(t)$-integral, and by replacing strains and displacements by strain rates and displacement rates, respectively. Based on this argument, authors [2,6] extended the J-A_2 three-term solution for elastic-plastic hardening materials to a three-term near-tip solution for a plane strain mode-I crack in power-

law creeping materials with two parameters: C-integral and a constraint parameter A_2. Hence, the three-term asymptotic fields under the steady-state creep are described by

$$\bar{\sigma}_{ij} = A_1\left[\bar{r}^{s1}\tilde{\sigma}_{ij}^{(1)}(\theta) + A_2\bar{r}^{s2}\tilde{\sigma}_{ij}^{(2)}(\theta) + A_3\bar{r}^{s3}\tilde{\sigma}_{ij}^{(3)}(\theta) + ...\right], \tag{1}$$

the same equation as those for elastic-plastic state, but with different amplitude factors A_1, A_2, A_3 . The angular functions of stress $\tilde{\sigma}_{ij}^{(k)}(\theta)$ in Eq.1 for creeping materials are the same as those for power-law hardening materials. In the case of the creeping material the first term amplitude factor A_1 can be obtained by replacing appropriate parameters [7]

$$A_1(t) = \left(C(t)/\left(\dot{\varepsilon}_0\sigma_0 I_n\right)\right)^{1/(n+1)} \tag{2}$$

where σ_0 is a reference stress, $\dot{\varepsilon}_0$ is a reference creep strain rate and n is the creep exponent. To complete the three-term asymptotic solution, it is necessary to calculate amplitude factor A_2. A few methods have been proposed for this pupose. In the present work, the stress components $\bar{\sigma}_{rr}$ and $\bar{\sigma}_{\theta\theta}$ of Eq.1 at $\theta = 0^\circ$ for different crack distance $\bar{r}$ are used to determine a value of A_2 by matching the three-trem solution with appropriate finite element results for $\bar{\sigma}_{rr}^{FEM}$ and $\bar{\sigma}_{\theta\theta}^{FEM}$. Thus, the stresses $\bar{\sigma}_{rr}, \bar{\sigma}_{\theta\theta}$ or some combinations of them, e.g. $(\bar{\sigma}_{\theta\theta}/\bar{\sigma}_{rr})$ can be used for fitting. Based on the stress asymptotic expansion 1, one has

$$\bar{\sigma}_{\theta\theta}/\bar{\sigma}_{rr} = \left(\bar{r}^{s_1}\tilde{\sigma}_{\theta\theta}^{(1)} + A_2\bar{r}^{s_2}\tilde{\sigma}_{\theta\theta}^{(2)} + A_2^2\bar{r}^{s_3}\tilde{\sigma}_{\theta\theta}^{(3)}\right)/\left(\bar{r}^{s_1}\tilde{\sigma}_{rr}^{(1)} + A_2\bar{r}^{s_2}\tilde{\sigma}_{rr}^{(2)} + A_2^2\bar{r}^{s_3}\tilde{\sigma}_{rr}^{(3)}\right). \tag{3}$$

Substituting the finite element stress component into the three-trem solution (1), one obtains the first term amplitude factor A_1

$$A_1^{FEM} = \bar{\sigma}_{\theta\theta}^{FEM}\Big/\left(\bar{r}^{s_1}\tilde{\sigma}_{\theta\theta}^{(1)} + A_2\bar{r}^{s_2}\tilde{\sigma}_{\theta\theta}^{(2)} + A_2^2\bar{r}^{s_3}\tilde{\sigma}_{\theta\theta}^{(3)}\right). \tag{4}$$

In this system of linear equations the governing paremeters are the second-term amplutude factor A_2 and ratio $\bar{\sigma}_{\theta\theta}^{FEM}/\bar{\sigma}_{rr}^{FEM}$.

The higher-order terms in Eq.1 control the deviation of the crack tip fields from the HRR solution. The intensity of this deviation, in terms of the value of A_2, in a cracked body depends on crack tip distance, the loading configuration, material properties and so on. Let us introduce the measure of such deviation, like Nikishkov [1] in form of the sum of second and third terms in Eq.1

$$Q_{\theta\theta} = A_1\left(A_2\bar{r}^{s_2}\tilde{\sigma}_{\theta\theta}^{(2)} + A_2^2\bar{r}^{s_3}\tilde{\sigma}_{\theta\theta}^{(3)}\right). \tag{5}$$

In all our calculations the angular stress distributions, the crack tip distance and the creep time are normalized as follows

$$\tilde{\sigma}_{e,max}^{FEM} = \left(\frac{3}{2}s_{ij}^{FEM}s_{ij}^{FEM}\right)_{max}^{1/2} = 1, \quad \tilde{\sigma}_{e,max}^{(k)} = \left(\frac{3}{2}s_{ij}^{(k)}s_{ij}^{(k)}\right)_{max}^{1/2} = 1, k = 1,2,3.$$

$$\bar{r} = \left(\sigma_0\dot{\varepsilon}_0 r/C\right) = (r/a)\Big/\left(\pi\sqrt{n}\left(\frac{\sqrt{3}}{2}\frac{\sigma}{\sigma_0}\right)^{n+1}\right), \quad \frac{t}{t_T} = \frac{t(n+1)EC}{(1-\nu^2)K_I^2}, \tag{6}$$

where K_I is stress intensity factor, ν is the Poisson's ratio, E is the Young's modulus, t is current creep time, t_T is the characteristic time for transition from small-scale creep to extensive creep [8].

Our attention in this work is focused on two-dimensional mode-I stationary crack problems under plane strain conditions. The Norton constitutive relation was employed to define the stress-strain rate curve corresponding to the purely power-law creeping material behavior

$$\dot{\varepsilon} = \dot{\varepsilon}_0 \left[\sigma/\sigma_0\right]^n \text{ or } \dot{\varepsilon} = B\sigma^n,\ B = \dot{\varepsilon}_0/\sigma_0^n . \tag{7}$$

For the present problem, the Young's modulus, Poisson's ratio and the yield stress were considered to be 205 GPa, 0.3 and 460 MPa, the creep parameter and the creep exponent are B=1.4·10^{-10} and n=3.

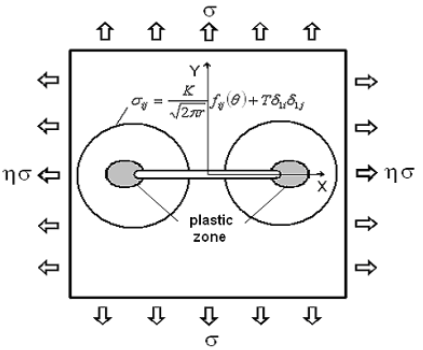

Fig.1. Biaxially loaded cracked panel.

The considered panel (Fig.1) was subjected to biaxial loading with three different biaxial stress state: eqiubiaxial tension-compression ($\eta = -1$), uniaxial tension ($\eta = 0$) and equibiaxial tension-tension ($\eta = +1$). Each type of biaxial loading is analyzed at nine stages of creep time which is varied from $t = 0$ up to $t = 5\cdot10^4$ hours. Our computations terminated at $t = 5\cdot10^4$ hours, which is the time when the creep zone radius equals about 80 percent of the plate outer boundary. Table 1 gives the values of creep time in both natural and dimensionless form.

Table 1. Values of varied creep time in numerical calculations for creeping material.

№	1	2	3	4	5	6	7	8	9
t [hours]	$1\cdot10^2$	$3\cdot10^2$	$5\cdot10^2$	$1\cdot10^3$	$3\cdot10^3$	$5\cdot10^3$	$1\cdot10^4$	$3\cdot10^4$	$5\cdot10^4$
t/t_T	0.0925	0.2775	0.4625	0.925	2.775	4.625	9.25	27.75	46.25

Results and Discussion

Radial stress distributions for creeping material

The tangential stress distributions $\overline{\sigma}_{\theta\theta}$ ahead of the crack-tip ($\theta = 0$) for three types of biaxial stress states are displayed in Figure 2 where the full-field solution stresses are normalized by the yield stress σ_y and the radial distance r is normalized by $C/(\sigma_0\dot{\varepsilon}_0)$. Numbering of lines in Figure 2 corresponds to the creep time in ascending order. This plot shows how both positive and negative biaxial loads affect the tangential stresses in mode I. Observe that the influence of creep time on the tangential full field stress distributions depends on the biaxial nominal stress state. In all calculations, the tangential stress behavior in the radial direction within $r/[C/(\sigma_0\dot{\varepsilon}_0) < 0.001]$ is

characterized as an evident unloading state, while beyond $r/[C/(\sigma_0\dot{\varepsilon}_0)>0.002]$ the radial stress distributions are approximately uniform. Note that in this region the stress gradient is depending on the biaxial stress state. Moreover, the change of stress gradients with respect to the creep time is large at $\eta=+1$ and is very small at $\eta=-1$. Thus, under the equibiaxial tension-compression stress state with $\eta=-1$ the full field tangential stress is nearly unaffected by the creep time when $r/[C/(\sigma_0\dot{\varepsilon}_0)>0.002]$.

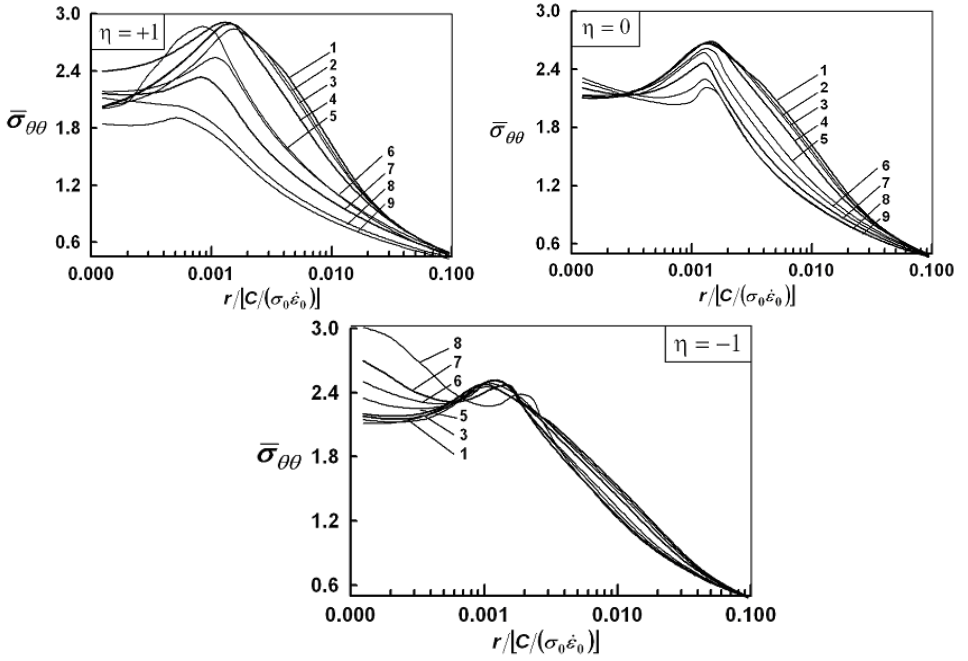

Fig. 2. Radial stress distributions along θ=0° under biaxial loading.

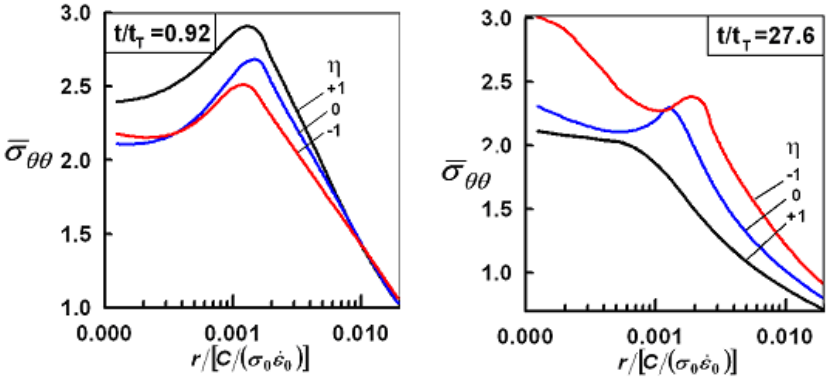

Fig. 3. Tangential stress redistribution on creep stages.

The general trend of the full field tangential stress redistribution in the radial direction under different biaxial stress state with respect to creep time is illustrated in Fig.3. It is interesting to note that at the short creep time $t/t_T = 0.92$ or small scale creep conditions, the maximum values of the tangential stresses correspond to the equibiaxial tension $\eta = +1$. At the transition creep time $2.76 > t/t_T > 0.92$ all stress distributions for different biaxial loading nearly coincide with each other. For long time $t/t_T = 27.6$ or extensive creep conditions already the equibiaxial tension-compression stress state $\eta = -1$ has maximal values of the tangential stresses within the region of considered crack tip distances. In summary, from small scale creep (i.e. $t < t_T$) to extensive creep (i.e. $t > 9.2t_T$), the equibiaxial tension and the equibiaxial tension-compression have contrary tendencies of changing in stress distributions. This is reasonable because under a constant remote loading, creep deformations leading to blunting and continuously evolving crack tip fields, will continue to accumulate with different intensity depending on biaxial stress state.

Angular stress distributions for creeping material

As well as in elastic-plastic material case, in order to background the validity of the three-term expansion 1, in this section the full field finite element results, HRR-type fields and the three-term asymptotic solutions are considered and compared for creeping material.

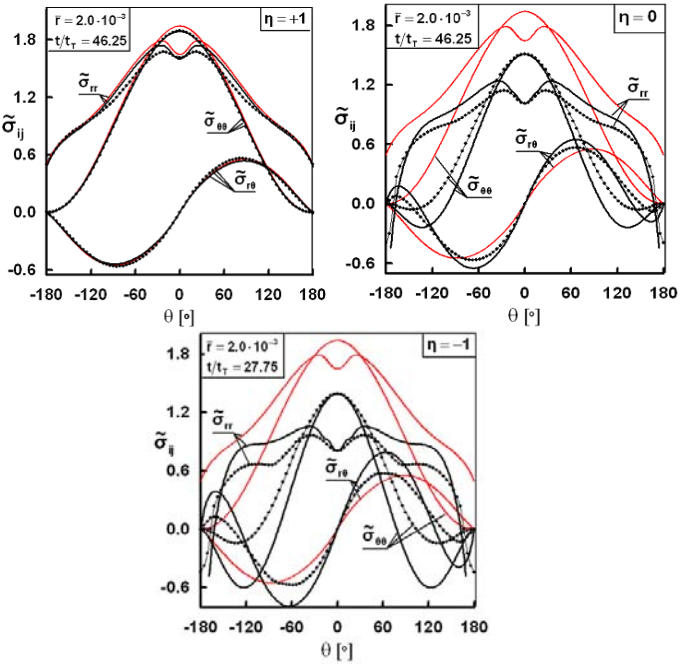

Fig. 4. Angular stress distributions under different biaxial stress states.

The full field finite element solution is indicated by the symbols while the HRR field is indicated by the thin solid line and the three-term solution by the thick line. Figure 4 shows angular distributions of the normal $\tilde{\sigma}_{rr}, \tilde{\sigma}_{\theta\theta}$ and shear $\tilde{\sigma}_{r\theta}$ stress components at the position from crack tip $r/[C/(\sigma_0 \dot{\varepsilon}_0)] = 2 \cdot 10^{-3}$ for different biaxial stress state at long creep time $t/t_T = 46.2$.

Near the crack tip within the finite strain or unloading zone neither the HRR field nor the three term asymptotic solution coincide with the finite element results. However, at a radial distance more

than the unloading zone $r/[C/(\sigma_0\dot{\varepsilon}_0)] = 2\cdot10^{-3}$ the three-term solutions are in good agreement with full field FEM results for the times considered here from $t/t_T = 0.46$ to $t/t_T = 46.2$. The quality of the approximation by a three-term expansion (1) is better in all interval of angular coordinate changing. The HRR-type fields deviate from both the FEM results and the higher-order term solutions for all the time except for the equibiaxial tension at $\eta = +1$. Although not shown here, for extensive creep when $9.2 < t/t_T < 46.2$ the same biaxial loading and crack distance effects similar to the creep time $t/t_T = 46.2$ were observed for the dimensionless stress components angular distributions.

Good agreement analytical findings with finite element results conforms again that HRR-solution corresponds only to the equibiaxial tension $\eta = +1$ which is particular case of general biaxial loading. The results and analyses of polar stress distributions indicate clearly that the three-term solution 1 is correct for all times from the small scale creep to the extensive creep.

Constraint parameter behavior for creeping material

Figure 5 is the variation of the amplitude A_1 and A_2 in the three-term asymptotic solution 1 as the function of the crack tip distance at different creeping stages under biaxial loading ($\eta = +1; 0; -1$). The results in this figure are obtained by Eqs 2,5 from the finite element analysis with the account of the three-term asymptotic solution with respect to the dimensionless higher-order stress components $\tilde{\sigma}_{rr}^{(k)}, \tilde{\sigma}_{\theta\theta}^{(k)}, \tilde{\sigma}_{r\theta}^{(k)}$ $(k = 1,2,3)$. In this figure the crack tip distance is normalized by $r/\rho = 10^3 r/[C/(\sigma_0\dot{\varepsilon}_0)]$, while the creep time is normalized by the transition time t_T.

In the case of the uniaxial tension $\eta = 0$ accounting for this value the amplitude A_1 from formula 2 is determined as $A_1 = 0.959$ and represented in Fig.5 as the corresponding plane. It is necessary to note that the analytical Riedel-Rice solution is only a particular case of our numerical results. It is found that the creep time has certain influence on A_2 only in short time within the finite strain zone. One can conclude that the amplitude A_2 in the three-term asymptotic solution for power-law creeping materials is approximately independent of the time at extensive creep conditions, i.e. the creep time has no role in the crack-tip stress fields. On the other hand, the distance from the crack tip has significant effect on the constraint parameter A_2 as shown in Fig.5.

The value of amplitude A_2 is negative for all the studied creep stages, and varies substantially with the biaxial loading. From comparison of different biaxial stress states it is clear that the general tendency is that the absolute value of A_2 decreases with change ratio η from +1 up to -1. Therefore, for a given creep time t/t_T and crack distance r/ρ, the loss of constraint is directly related to A_2 by means of biaxial stress ratio η. As pointed out previously for elastic-plastic material, again in creeping material the value of A_2 approximately achieves zero under equibiaxial tension at $\eta = +1$ that confirms the undertone of the HRR-type solution.

Because the validity of all mentioned above concepts depends on the chosen reference field a local parameter of crack tip constraint and stress triaxiality is proposed by Henry and Luxmoore [9] as a secondary fracture parameter

$$h(r,\theta,z) = \sigma_{kk} \Big/ \left(3\sqrt{\frac{3}{2} s_{ij} s_{ij}} \right). \tag{8}$$

where σ_{kk} and s_{ij} are hydrostatic and deviatiric stresses, respectively. Being the function of both first invariant of the stress tensor and the second invariant of the stress deviator, it is a local measure of in-plane and out-of-plane constraint effects that is independent of any reference field. Figure 6 depicts the variations of the constraint parameter h with the distance from the crack tip at the two creep stages under biaxial loading. One can conclude that for power-law creeping material within the unloading zone, the stress triaxiality parameter h is approximately independent on the stress biaxiality at both small scale and extensive creep. The finite-strain effect on the triaxiality stress is

not significant at the crack distance $r/[C/(\sigma_0\dot{\varepsilon}_0)] < 1\cdot10^{-3}$. Beyond this distance the strong dependence of h on load biaxiality can be seen. It should be noted that only at the short creep time $t/t_T < 0.92$, the triaxiality stress distributions are similar while they become more different with increasing creep time t/t_T. The general tendency is that the absolute value of h for the equibiaxial tension $\eta = +1$ increases drastically with t/t_T, whereas the values of h for other biaxial stress state, i.e. $\eta = 0$ and $\eta = -1$ do not.

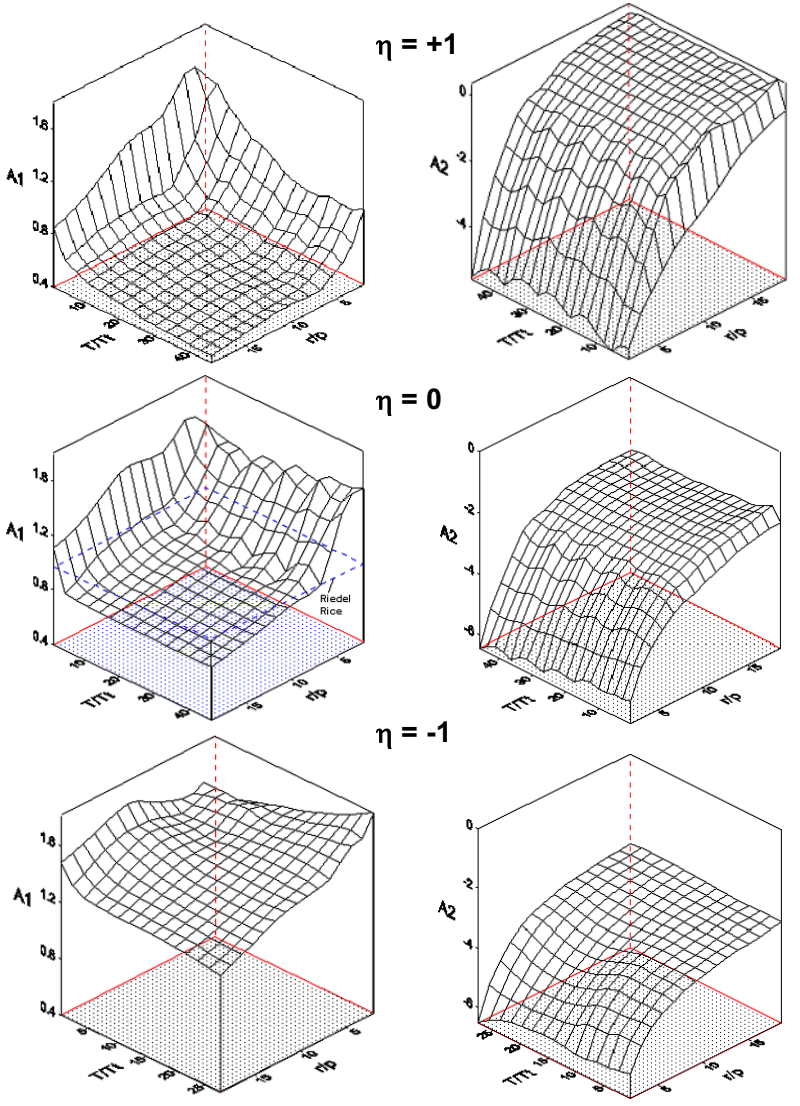

Fig. 5. Amplitude factors behavior under biaxial loading.

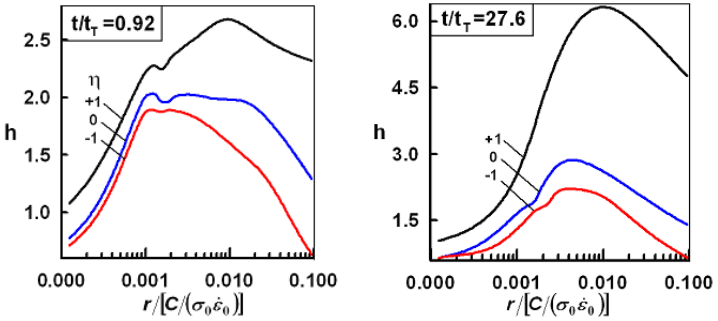

Fig. 6. Stress triaxiality parameter distributions on creep stages.

Conclusions

The higher-order asymptotic crack-tip fields are investigated in the present work for a plane strain mode I crack in creeping material under the biaxial loading conditions. Good agreement analytical findings on the base of the three-term expansion with finite element results conforms that HRR-solution for creeping material is particular case of general biaxial loading which corresponds to the equibiaxial tension. Several constraint concepts are analyzed with respect to their capability of characterizing load biaxiality effect. It is found that the influence of the nominal biaxial stress state is realized only through the higher-order terms which have a sense of the constraint parameters in different approaches. Because quantum of the sum of the second and the third terms in asymptotic expansion can be average up to 52-58 % with respect to the first HRR-type term under generally biaxial stress states the necessity to include the higher-order terms solution for characterizing constraint effects under biaxial loading is clear.

References

[1] G.P. Nikishkov: Engineering Fracture Mechanics Vol. 50 (1995), pp. 65-83.

[2] B.N. Nguyen, P.R. Onck, E. van der Giessen: Journal of Applied Mechanics Vol. 67 (2000), pp. 372-382.

[3] N.P. O'Dowd and C.F. Shih: Journal of the Mechanics and Physics of Solids Vol. 39 (1991), pp. 989-1015.

[4] H. Yuan and W. Brocks: Journal of the Mechanics and Physics of Solids Vol. 46 (1998) pp. 219-241.

[5] N.J. Hoff: Quarterly Applied Mechanics Vol. 12 (1954), pp. 49-55.

[6] Y.J. Chao, X.K. Zhu, L. Zhang: International Journal of Solids and Structures Vol. 38 (2001), pp. 3853-3875.

[7] H. Riedel, J.R. Rice: American Society for Testing and Materials, ASTM STP 700 (1980), pp. 112-130.

[8] F.Z. Li, A. Needleman, C.F. Shih: International Journal of Fracture Vol. 36 (1988), pp. 163-186.

[9] B.S. Henry, A.R. Luxmoore: Engineering Fracture Mechanics Vol. 57 (1997), pp. 375-390.